JOURNAL OF AIRCRAFT
Vol. 30, No. 6, Nov.–Dec. 1993

Finite Element Nonlinear Flutter and Fatigue Life of Two-Dimensional Panels with Temperature Effects

David Y. Xue* and Chuh Mei†
Old Dominion University, Norfolk, Virginia 23529

A frequency domain method for two-dimensional nonlinear panel flutter with thermal effects obtained from a consistent finite element formulation is presented. von-Karman nonlinear strain-displacement relation is used to account for large deflections, and the quasisteady first-order piston theory is employed for aerodynamic loading. The panel motion under a combined thermal-aerodynamic loading can be mathematically separated into two parts and then solved in sequence: 1) thermal-aerodynamic static deflection (time-independent equilibrium position), and 2) limit-cycle oscillations. The finite element frequency domain results are compared with numerical time domain solutions. In a limit-cycle motion, the panel frequency and stress can be determined, thus fatigue life can be predicted. The influence of temperature and dynamic pressure on panel fatigue life is presented. Endurance and failure dynamic pressures can be established at a given temperature from the present method.

Nomenclature

$[a_a]$, $[A_a]$ = element and system aerodynamic influence matrices
c = maximum of $\{W\}_t$
D = bending rigidity, $Eh^3/12(1-\nu^2)$
E = Young's modulus
g_a = nondimensional aerodynamic damping
$[g]$, $[G]$ = element and system aerodynamic damping matrices
h = plate thickness
$[k]$, $[K]$ = element and system stiffness matrices
l, L = element and plate lengths
M_∞ = Mach number
$[m]$, $[M]$ = element and system mass matrices
N = cycles to failure
$[n1]$, $[n2]$, $[N1]$, $[N2]$ = element and system nonlinear stiffness matrices
$\{p\}$, $\{P\}$ = element and system force vectors
q = dynamic pressure, $\rho_a V^2/2$
u, w = element displacement functions
V = airflow speed
$\{w\}$, $\{W\}$ = element and system nodal displacements
x, z = coordinate axes
α = panel damping rate or coefficient of thermal expansion
β = $\sqrt{M_\infty^2 - 1}$
ε = total strain
κ = eigenvalue
λ = nondimensional dynamic pressure, $2qL^3/\beta D$
ν = Poisson's ratio
ρ = mass density
σ = stress
$\{\phi\}$ = mode shapes
Ω = complex panel motion parameter, $\alpha + i\omega$
ω = frequency

Subscripts

a = air, alternate
b = bending
cr = critical
e = endurance
f = failure
l = limit-cycle
m = mean, membrane
s = static
t = time-dependent, tensile
ΔT = thermal

Introduction

THE panel flutter phenomenon, a self-excited oscillation in supersonic flow, has been studied experimentally and analytically for decades.[1–20] Small-deflection linear theory establishes that there is a critical dynamic pressure (or airflow speed) beyond which the panel motion becomes unstable. However, the panel flutter experiments[2,3] showed that the panel oscillations are stable and independent from initial conditions. This motion is called limit-cycle oscillation and large-deflection nonlinear theory is required to predict such motion. Surveys on panel flutter have been given by Dowell,[4] and recently by Reed et al.[5] In analytical studies, a number of methods exists for the investigation of limit-cycle oscillations of panel behavior, e.g., harmonic balance,[6,7] perturbation,[8,9] time numerical integration,[10,11] and finite element[12–17] methods. In most studies, the effects of uniform temperature are treated as an equivalent mechanical loading.

Few flutter analyses have dealt with thermal loading directly.[1,18–20] Due to the development of high supersonic flight vehicles, such as the National Aero-Space Plane and High Speed Civil Transport, the thermal effects and an efficient and accurate finite element flutter analysis is required to meet the needs for designing complex panels. The thermal environment can affect panel motions by introducing thermal in-plane forces and thermal bending moments, and altering material properties. Although mechanical loading could simulate some simple temperature distributions, thermal stress analysis is necessary since simple mechanical loading cannot be sub-

Presented as Paper 91-1170 at the AIAA 32nd Structures, Structural Dynamics, and Materials Conference, Baltimore, MD, April 8–10, 1991; received Aug. 16, 1991; revision received Aug. 20, 1992; accepted for publication Sept. 10, 1992.

*Research Associate, Department of Mechanical Engineering and Mechanics. Member AIAA.

†Professor, Department of Mechanical Engineering and Mechanics. Associate Fellow AIAA.

stituted for a complex temperature distribution. According to the authors' knowledge, there is no analytical study available in the literature on nonlinear panel flutter with nonuniform temperature distributions using finite element methods. This research is focused on developing a consistent finite element formulation and solution procedure for nonlinear panel flutter with effects of temperature. The present finite element procedure is a frequency domain solution based on the panel undergoing limit-cycle oscillations. The finite element system differential equation contains a time-independent loading due to temperature; so that the solution of total panel motion is the sum of a time-independent static equilibrium position (particular solution) and a time-dependent dynamic oscillation (homogeneous solution). Both the static equilibrium position and the dynamic oscillation are considered to be large. The static equilibrium solution gives stability boundaries which distinguishes panel behavior into five regions: 1) flat panel, 2) buckled panel, 3) harmonic motion, 4) periodic (nonharmonic) motion, and 5) chaotic motion. The dynamic solution, on the other hand, gives dynamic stability boundaries and limit-cycle responses. The finite element limit-cycle results are compared with time domain solutions. In the iterative solution procedure, the nonlinear stiffness matrices are re-evaluated for the updated panel deflection and the nonlinear time functions are approximated by a simple harmonic function.[17,21] In limit-cycle motions, panel frequency and amplitude can be determined uniquely (independent from initial conditions) for given sets of temperature and dynamic pressure. Therefore, the cyclic stress can be calculated. By applying certain fatigue analysis method, i.e., Heywood's approach,[22] the fatigue life of a panel can be estimated. Examples of fatigue life estimation are given in this article. A dynamic pressure vs fatigue life (λ-H curve) relation is presented for panel fatigue life analysis, and interesting endurance and failure dynamic pressures can be found for each different temperature. This may aid in practical panel design.

Finite Element Formulation

Consider the flat panel of L, h, and ρ, with air flowing above the panel at M_∞ and a temperature change $\Delta T(x)$, shown in Fig. 1. It is assumed that the air flowing above the panel is in the positive x direction and that the effects of the cavity on the back side of the panel can be neglected.

For an isotropic Hookean material under a state of plane stress and subjected to $\Delta T(x)$, the stress-strain and strain-displacement relations for a thin two-dimensional plate ($\varepsilon_x = \varepsilon$, $\varepsilon_y = 0$) are

$$\sigma = \frac{E}{1-\nu^2}\varepsilon - \frac{\alpha E}{1-\nu}\Delta T(x) \tag{1}$$

$$\varepsilon = u_{,x} + \tfrac{1}{2}w_{,x}^2 - zw_{,xx} \tag{2}$$

where E, ν, and thermal expansion coefficient α could be temperature-dependent. The quasisteady first-order piston theory[23] is employed for aerodynamic loading. By applying the principal of virtual work, the equations of motion for a two-dimensional plate element subjected to a simultaneous $\Delta T(x)$ and λ can be derived as

$$\frac{1}{\omega_0^2}\begin{bmatrix}[m_b] & 0\\ 0 & [m_m]\end{bmatrix}\begin{Bmatrix}\ddot{w}_b\\ \ddot{w}_m\end{Bmatrix} + \frac{g_a}{\omega_0}\begin{bmatrix}[g] & 0\\ 0 & 0\end{bmatrix}\begin{Bmatrix}\dot{w}_b\\ \dot{w}_m\end{Bmatrix} + \lambda\begin{bmatrix}[a_a] & 0\\ 0 & 0\end{bmatrix}\begin{Bmatrix}w_b\\ w_m\end{Bmatrix} + \left(\begin{bmatrix}[k_b] - [k_{N\Delta T}] & 0\\ 0 & [k_m]\end{bmatrix} + \frac{1}{2}\begin{bmatrix}[n1_{Nu}] & [n1_{bm}]\\ [n1_{mb}] & 0\end{bmatrix} + \frac{1}{3}\begin{bmatrix}[n2_b] & 0\\ 0 & 0\end{bmatrix}\right)\begin{Bmatrix}w_b\\ w_m\end{Bmatrix} = \begin{Bmatrix}0\\ p_{m\Delta T}\end{Bmatrix} \tag{3}$$

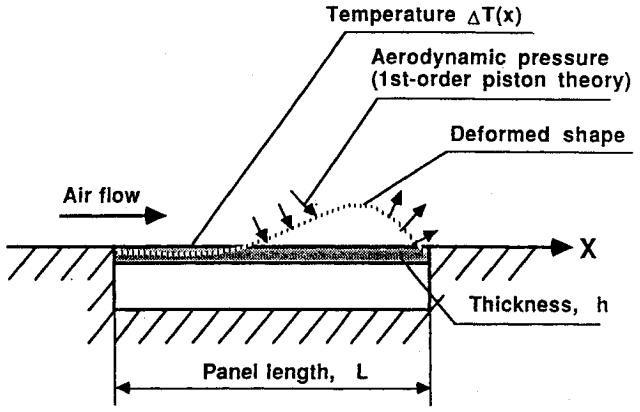

Fig. 1 Panel geometry.

where the element matrices and thermal load vector are derived in detail,[1] and the dynamic pressure $\lambda = 2qL^3/\beta D$ and aerodynamic damping $g_a = \rho_a V(M_\infty^2 - 2)/\beta^3\rho h\omega_0$ are nondimensional parameters, and $\omega_0 = (D/\rho hL^4)^{1/2}$ is a reference frequency.

System Equations and Solution Procedures

Summing up the contributions from all the elements and taking account of the boundary conditions, the system equations of motion can be expressed in matrix form as

$$(1/\omega_0^2)[M]\{\ddot{W}\} + (g_a/\omega_0)[G]\{\dot{W}\} + \lambda[A_a]\{W\} + [K - K_{N\Delta T} + \tfrac{1}{2}N1 + \tfrac{1}{3}N2]\{W\} = \{P_{\Delta T}\} \tag{4}$$

where $[K_{N\Delta T}]$ is the system geometric stiffness due to thermal stress resultant $N_{\Delta T}$, $[N1]$ and $[N2]$ are the first- and second-order nonlinear system stiffness matrices which depend linearly and quadratically upon $\{W\}$, $\{P_{\Delta T}\}$ is the system thermal load vector, and $\{W\}^t = [\{W_b\}^t, \{W_m\}^t]$. Equation (4) is a set of differential equations with respect to time t, and the right side force term is independent of t. A mathematic treatment is to assume that the solution is the sum of a time-dependent homogeneous solution and a time-independent particular solution. For this problem, the homogeneous solution refers to a self-excitated dynamic oscillation, $\{W\}_t$, and the particular solution refers to a static equilibrium thermal-aerodynamic deflection, $\{W\}_s$, as

$$\{W\} = \{W\}_s + \{W\}_t \tag{5}$$

where both deflections $\{W\}_s$ and $\{W\}_t$ are considered to be large. Substituting Eq. (5) into Eq. (4), Eq. (4) can be separated into two equations

$$\lambda[A_a]\{W\}_s + ([K] - [K_{N\Delta T}] + \tfrac{1}{2}[N1]_s + \tfrac{1}{3}[N2]_s)\{W\}_s = \{P_{\Delta T}\} \tag{6}$$

$$(1/\omega_0^2)[M]\{\ddot{W}\}_t + (g_a/\omega_0)[G]\{\dot{W}\}_t + \lambda[A_a]\{W\}_t + ([K] - [K_{N\Delta T}] + [N1]_s + [N2]_s)\{W\}_t + ([N2]_{st} + \tfrac{1}{2}[N1]_t + \tfrac{1}{3}[N2]_t)\{W\}_t = 0 \tag{7}$$

The subscripts s and t, denote that the corresponding nonlinear stiffness matrix is evaluated using $\{W\}_s$ or $\{W\}_t$. Close examination of Eqs. (6) and (7), reveals that 1) Eq. (6) is a set of nonlinear algebraic equations and Eq. (7) is a set of nonlinear differential equations; 2) there is coupling between aerodynamic pressure ($\lambda[A_a]$, $g_a[G]$) and thermal loading ($[K_{N\Delta T}]$, $\{P_{\Delta T}\}$); and 3) Eq. (6) has to be solved first to determine $\{W\}_s$, the $\{W\}_t$ can then be found from Eq. (7).

Thermal/Aerodynamic Postbuckling Deflection

Equation (6) can be referred as a postbuckling problem with the effects of a set of combined dynamic pressure λ and temperature ratio $\Delta T(x)/\Delta T_{cr}$ (where $\Delta T(x)$ is the temperature change and ΔT_{cr} is the critical buckling temperature). It can be solved by using the Newton-Raphson iterative method for the ith iteration as

$$\{W_{i+1}\}_s = \{W_i\}_s + \{\Delta W_i\}_s \tag{8}$$

where the $\{\Delta W_i\}_s$ is determined from

$$[K]_{\tan}\{\Delta W_i\}_s = \{\Delta P_i\} \tag{9}$$

and the tangent stiffness matrix is given by

$$[K]_{\tan} = \lambda[A_a] + [K] - [K_{N\Delta T}] + [N1_i]_s + [N2_i]_s \tag{10}$$

$$\{\Delta P_i\} = \{P_{\Delta T}\} - (\lambda[A_a] + [K] - [K_{N\Delta T}] + \tfrac{1}{2}[N1_i]_s + \tfrac{1}{3}[N2_i]_s)\{W_i\}_s \tag{11}$$

The detailed procedure has been given in Ref. 1.

Critical Dynamic Pressure and Flutter Boundary

After obtaining $\{W\}_s$ from Eq. (6), the critical dynamic pressure of the aerodynamic/thermally loaded panel can be determined from Eq. (7) by dropping the nonlinear terms and neglecting the effects of inplane inertia as

$$\kappa[M_b]\{\phi\} = [K]_{\text{lin}}\{\phi\} \tag{12}$$

where the nondimensional κ and linear flutter stiffness matrix are

$$\kappa = -\left(\frac{\Omega}{\omega_0}\right)^2 - g_a\frac{\Omega}{\omega_0} \tag{13}$$

$$[K]_{\text{lin}} = \lambda[A_a] + [K_b] - [K_{N\Delta T}] + [N1_{Nu}]_s + [N2_b]_s - [N1_{bm}]_s[K_m]^{-1}[N1_{mb}]_s \tag{14}$$

The critical dynamic pressure λ_{cr} is the pressure which makes the coalescence of the first and second eigenvalues κ_1 and κ_2.

Limit-Cycle Amplitude—Dynamic Pressure Relation

The dynamic equation, Eq. (7), is solved by using the linearized updated mode with nonlinear time function (LUM/NTF) approximation.[17,21] This method assumes a simple harmonic solution by neglecting the higher harmonics, since the higher harmonic terms normally have a small influence on responses. Thus, the large-amplitude panel flutter with $\Delta T(x)$ becomes an iterative and linearized eigenproblem

$$\kappa_j[M_b]\{\phi_j\} = ([K]_{\text{lin}} + [\bar{K}_j])\{\phi_j\} \tag{15}$$

where the linearized stiffness matrix is

$$[\bar{K}_j] = (\sqrt{2}c/2)(-[N1_{bm}]_s[K_m]^{-1}\tfrac{1}{2}[\overline{N1_{mb}}]_t + \tfrac{1}{2}[\overline{N1_{Nu1}}]_t + [\overline{N2_b}]_{st} - \tfrac{1}{2}[\overline{N1_{bm}}]_t[K_m]^{-1}[N1_{mb}]_s) + (3c^2/4)(\tfrac{1}{2}[\overline{N1_{Nu2}}]_t + \tfrac{1}{3}[\overline{N2_b}]_t - \tfrac{1}{2}[\overline{N1_{bm}}]_t[K_m]^{-1}\tfrac{1}{2}[\overline{N1_{mb}}]_t) \tag{16}$$

Detailed matrix expressions are given in Refs. 1 and 17. For a given maximum deflection ($c = \max\{W\}_t$), the limit-cycle dynamic pressure λ_l is determined by coalescence of the two lowest eigenvalues κ_1 and κ_2.

Fatigue Life Estimation

In flutter experiments, it has been observed that many panels failed before the steady-state flutter motions were reached. It could be considered that fatigue plays an important role in failure of such panels.[24] In a fatigue analysis, stresses and failure cycles are the basic parameters. The panel failure cycles N is related to the panel frequency. For general nonlinear structural vibration, the displacement and the frequency are related to each other; thus, the stress level and failure cycles N are coupled. They are determined by initial conditions for free vibrations and dominated by the input force for steady-state forced vibrations. In panel flutter limit-cycle motions, the dynamic equations of motion, Eq. (7), are similar to those for a free vibration problem, but the responses are independent from the initial conditions. How do these features affect fatigue analysis? This question is addressed by the following.

Stress Representation

The stress expression, Eq. (1), can be rewritten in terms of panel displacements as

$$\sigma = \frac{E}{1-\nu^2}\left[u_{,x} + \frac{1}{2}w_{,x}^2 - zw_{,xx}\right] - \frac{\alpha E}{1-\nu}\Delta T(x) \tag{17}$$

Substituting the expression for $\{W\}$ from Eq. (5) into Eq. (17), the stress can be separated to three parts

$$\sigma = \frac{E}{1-\nu^2}\left[(u_t + u_s)_{,x} + \frac{1}{2}(w_t + w_s)_{,x}^2 - z(w_t + w_s)_{,xx}\right] - \frac{\alpha E}{1-\nu}\Delta T(x) = \sigma_1 + \sigma_2 + \sigma_3 \tag{18}$$

where

$$\sigma_1 = \frac{E}{1-\nu^2}\left[u_{t,x} + \frac{1}{2}w_{t,x}^2\right] \tag{19a}$$

$$\sigma_2 = \frac{E}{1-\nu^2}[-zw_{t,xx} + w_{t,x}w_{s,x}] \tag{19b}$$

$$\sigma_3 = \frac{E}{1-\nu^2}\left[u_{s,x} + \frac{1}{2}w_{s,x}^2 - zw_{s,xx}\right] - \frac{\alpha E}{1-\nu}\Delta T(x) \tag{19c}$$

The stress component σ_1 is a time-dependent stretching stress, σ_2 is a time-dependent bending stress, and σ_3 is a static stress. For a harmonic limit-cycle oscillation, the thermal-aerodynamic deflection of the panel is zero ($\{W\}_s = 0$), and the stress components become

$$\sigma_1 = \frac{E}{1-\nu^2}\left[u_{t,x} + \frac{1}{2}w_{t,x}^2\right] \tag{20a}$$

$$\sigma_2 = \frac{E}{1-\nu^2}(-zw_{t,xx}) \tag{20b}$$

$$\sigma_3 = -\frac{\alpha E}{1-\nu^2}\Delta T(x) \tag{20c}$$

Heywood's Fatigue Approach

The fatigue life analysis of various aircraft materials has been studied in Ref. 25, and Heywood's engineering approach was applied to common aluminum alloys. This approach[22] is based on testing and can be expressed as

$$\sigma_a = \pm\sigma_t[1 - \sigma_m/\sigma_t][A_0 + \gamma(1 - A_0)] \quad \text{(ksi)} \tag{21}$$

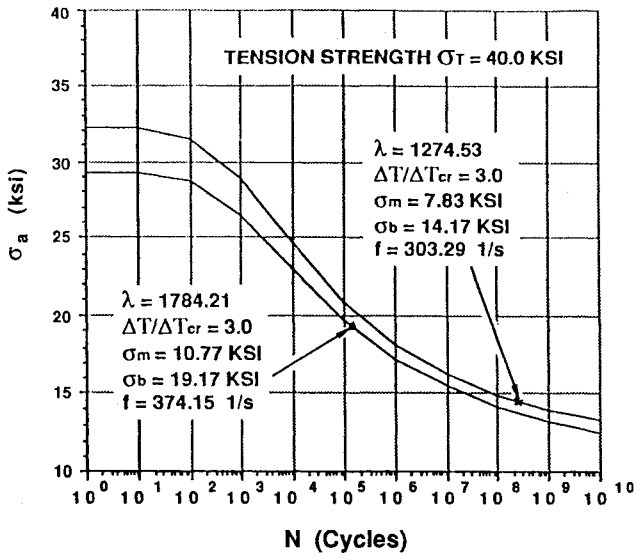

Fig. 2 Heywood's σ_a-N curve [Eq. (21)].

where

$$A_0 = [1 + 0.0031n^4/(1 + 0.045\sigma_t)]/(1 + 0.0031n^4)$$

$$\gamma = (\sigma_m/\sigma_t)/[1 + (\sigma_t n/320)^4]$$

$$n = \log(N)$$

In Eq. (21) σ_a (ksi) is the alternating stress, σ_t (ksi) is the temperature-dependent ultimate tensile strength of the material, and σ_m (ksi) is the mean stress and N is the number of cycles to failure. Equation (21) can be used to estimate the fatigue characteristics of an aluminum alloy panel knowing any three of the parameters σ_a, σ_m, N, or σ_t and solving for the fourth parameter. In the common fatigue analysis, Eq. (21) is plotted as a σ_a-log N(S-N) or σ_a-σ_m (Goodman diagram) curve. For example, Fig. 2 shows the σ_a-log N curve at σ_m = 7.83 ksi (and Fig. 3.5 of Ref. 22 for σ_a-σ_m curve) at σ_t = 40 ksi.

Dynamic Pressure vs Fatigue Life

In panel flutter fatigue analysis, it is inconvenient to use σ_a-log (N) or σ_a-σ_m curve, since σ_a and σ_m are related to frequency for a certain panel, and they are determined uniquely at a given temperature and dynamic pressure. That is, a panel under varying λ would have different σ_a-log (N) or σ_a-σ_m curves, and on each curve only one point (σ_a, σ_m, N) suits the panel behavior. On the other hand, N may not be a clear measure of service life, since for the same N the related frequencies will give different life quantities. By applying Heywood's approach and transferring life cycles N to lifetime hours H for the stresses associated with various flutter dynamic pressures λ, a λ-H curve (flutter dynamic pressure vs failure hours) can be plotted for a certain panel at a given temperature. An endurance dynamic pressure can also be determined. This is important information for panel design.

Results and Discussion

The present finite element method is applied to a simply supported panel with immovable inplane edges [$u(0) = u(L) = 0$] subjected to a combined airflow and temperature. The solution procedure is divided into two steps: 1) a static equilibrium solution from Eq. (6), and 2) a limit-cycle oscillation from Eq. (7). The first step has been studied in detail in Ref. 1. For the sake of completeness, some of the results are included here.

The two-dimensional plate considered is aluminum with the properties and dimensions: $E = 10.4 \times 10^6$ psi, $\nu = 0.3$, $\alpha = 12.9 \times 10^{-6}$ in./in./°F, $h = 0.064$ in., $L = 12$ in., and $\rho = 261.658 \times 10^{-6}$ lb-s^2/in.^{4} All of the finite element results presented in this study are for 12-element solutions required for convergence in Ref. 1.

Comparison with Time-Domain Solutions

A comparison was first made with Dowell's six-mode limit-cycle oscillation results (Fig. 8 of Ref. 10), obtained by numerical time integration. However, since the finite element formulation presented here differs slightly from the formulation presented in Ref. 10, the finite element inplane stiffness matrices were scaled by $(1 - \nu^2)$ to correlate with Eq. (1.4) of Ref. 10. This comparison is shown in Fig. 3 for several uniform temperature changes $\Delta T/\Delta T_{cr}$ ($= -R_x/\pi^2$ in Ref. 10) of 0, 1, 2, and 3. The finite element results using the LUM/NTF linearizing method agree extremely well with Dowell's results.

Arbitrary Temperature Distribution

To investigate the effects of temperature on panel flutter behavior, uniform temperature change $\Delta T = T_0$ and symmetric sinusoidal temperature variation along panel length $\Delta T(x) = T_1 \sin \pi x/L$ have been considered as the two tem-

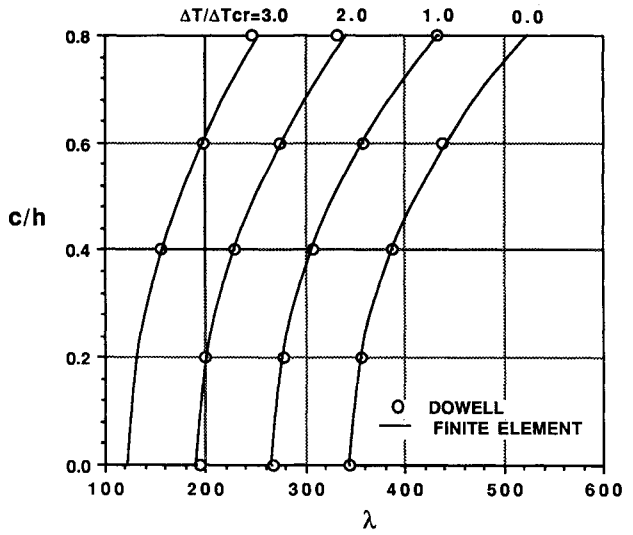

Fig. 3 Comparison of finite element and numerical time integration (six modes) limit-cycle results for a simply supported panel.

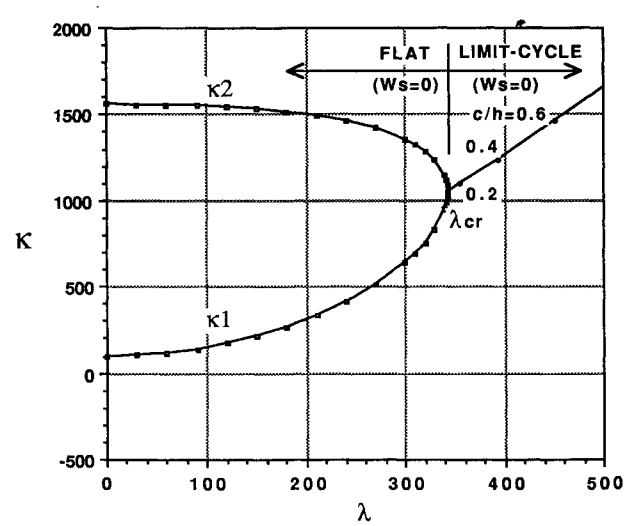

Fig. 4 Eigenvalue and limit-cycle amplitude vs dynamic pressure for a simply supported panel at $\Delta T(x)/\Delta T_{cr} = 0$.

perature distributions. Similar conclusions as those in Ref. 1 are obtained, i.e., for two different temperature distributions 1) $\Delta T_1(x)$ and 2) $\Delta T_2(x)$, if their temperature ratios are the same

$$\frac{\Delta T_1(x)}{\Delta T_{cr1}(x)} = \frac{\Delta T_2(x)}{\Delta T_{cr2}(x)} \tag{22}$$

then their limit-cycle dynamic pressures λ_l, limit-cycle eigenvalues κ_l (or panel frequencies of vibration), and limit-cycle panel amplitudes w_t are identical, but not the inplane displacements.

Eigenvalue and Amplitude vs Dynamic Pressure

Dynamic response of an aerothermally buckled panel can be obtained by solving the eigenproblems of Eqs. (12) and (15) for critical dynamic pressure and limit-cycle motions. The influence of temperature on eigenvalue variation vs dynamic pressure for a simply supported panel is shown in Figs. 4–6. In Fig. 4, the coalescence of the first and second eigenvalues occurs at $\lambda_{cr} = 343.45$ for $\Delta T(x)/\Delta T_{cr} = 0$. Classical analytical methods established coalescence at 343.36. Thus, finite element results compared extremely well with classical solutions. Limit-cycle oscillations occur for $\lambda > \lambda_{cr}$ with increasing amplitude as λ_l increases. The maximum dynamic deflection

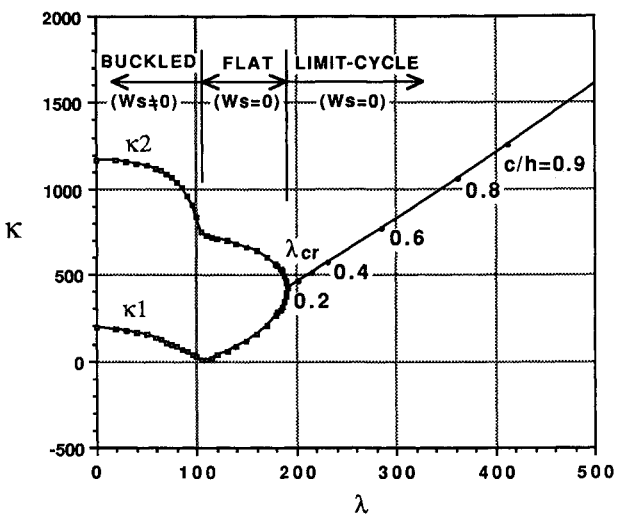

Fig. 5 Eigenvalue and limit-cycle amplitude vs dynamic pressure for a simply supported panel at $\Delta T(x)/\Delta T_{cr} = 2.0$.

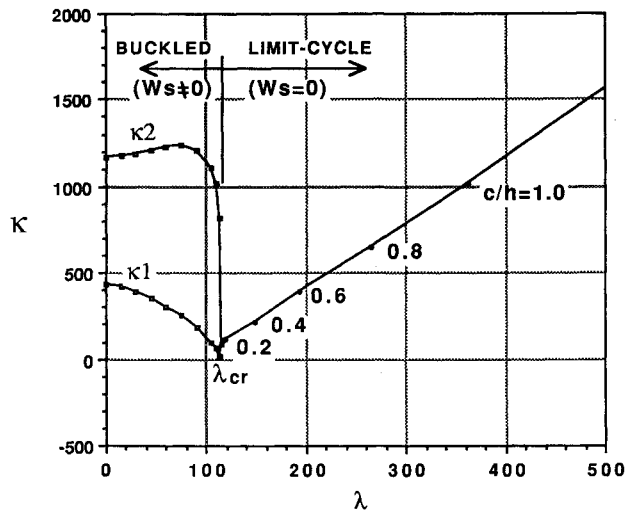

Fig. 6 Eigenvalue and limit-cycle amplitude vs dynamic pressure for a simply supported panel at $\Delta T(x)/\Delta T_{cr} = 3.2$.

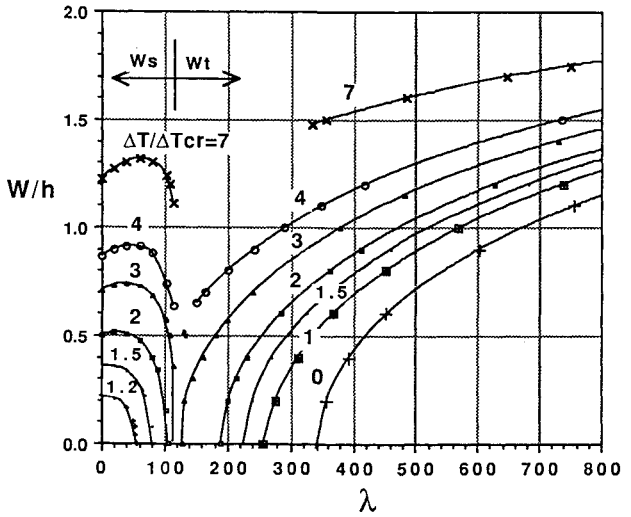

Fig. 7 Maximum deflection vs dynamic pressure for a simply supported panel at various $\Delta T(x)/\Delta T_{cr}$.

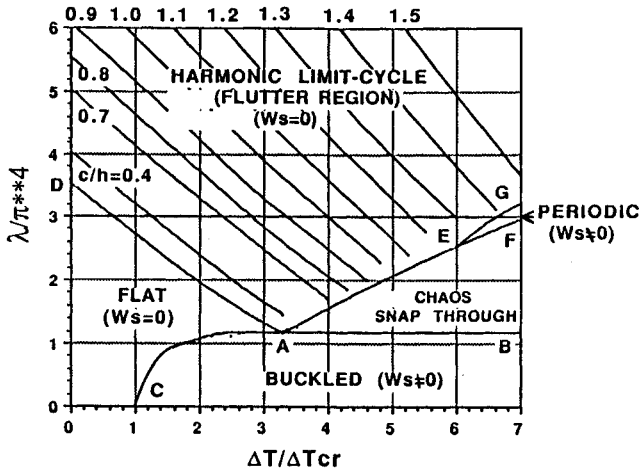

Fig. 8 Static-stability and flutter boundaries, and limit-cycle amplitudes for a simply supported panel.

W_t/h (or c/h at $x = 3L/4$) of 0.2, 0.4, and 0.6 are also marked on the limit-cycle curve.

The effect of temperature on panel flutter behavior are shown in Figs. 5 and 6. In Fig. 5, the critical dynamic pressure drops drastically down to $\lambda_{cr} = 190.92$ at $\Delta T(x)/\Delta T_{cr} = 2.0$. The panel is thermally buckled at $\Delta T(x)/\Delta T_{cr} = 2.0$ and $\lambda = 0$. As λ is increased, the aerothermally buckled deflection $\{W\}_s$ and κ_1 and κ_2 are all decreasing. When λ reaches the value of 103.35, the panel becomes flat and the lowest κ_1 is zero. As λ is further increased, the panel remains flat and the two eigenvalues approach one another and they finally coalesce at $\lambda_{cr} = 190.92$. As λ is increased beyond the critical value, limit-cycle panel motions occur.

In Fig. 6, the critical dynamic pressure reduces to the smallest $\lambda_{cr} = 114.163$ at $\Delta T(x)/\Delta T_{cr} = 3.2$. The panel is thermally buckled at $\Delta T(x)/\Delta T_{cr} = 3.2$ and $\lambda = 0$. As λ is increased, the aerothermally buckled panel flattens out. When λ reaches λ_{cr}, the panel deflection, κ_1 and κ_2 are all zero. As λ is increased further from the critical value, the panel goes immediately to limit-cycle motions. This $\Delta T(x)/\Delta T_{cr} = 3.2$ and $\lambda = 114.163$ is a very special temperature-dynamic pressure pair such that four regions of different panel motions (flat, buckled, limit-cycle, and chaotic) all intersect at this single point A as indicated in Fig. 8. The limit-cycle amplitudes $c/h = 0.2$, 0.4, 0.6, 0.8, and 1.0 (they are also the total panel

deflections due to $\{W\}_s = 0$) are shown on the limit-cycle curve.

The total deflection W/h (at $x = 0.75L$) vs λ with different $\Delta T(x)/\Delta T_{cr}$ are plotted in Fig. 7. The set of curves on the left side is obtained from Eq. (6). Since at that time λ has not reached the critical value and the flutter (limit-cycle oscillation) has not started ($W_t = 0$). On the other hand, the set of curves at the right side is obtained from Eq. (7) only, since at that stage the panel has been blown flat ($W_s = 0$). The discontinuities of the curves at temperature ratios over 3.2 (e.g., $\Delta T(x)/\Delta T_{cr} = 4$ or 7) are due to the chaotic area (Fig. 8). It can be considered that the chaotic motions are bounded with a static deflection $W_s/h \leq 1.1$ and a dynamic amplitude $W_t h \leq 1.5$ for temperature ratio of 7, and both W_s/h and W_t/h are within 0.65 for temperature ratio of 4.

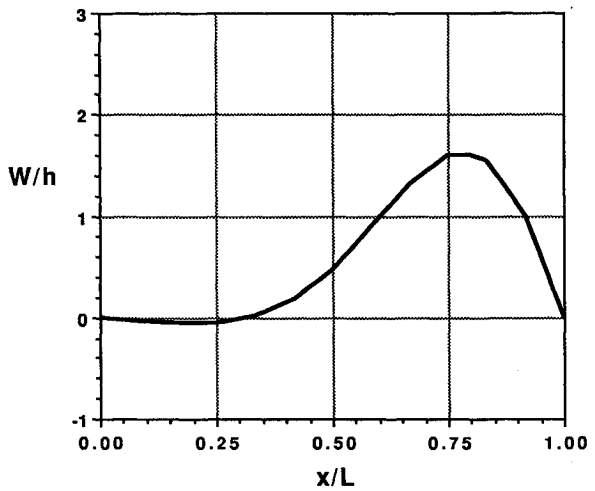

Fig. 9 Limit-cycle deflection of a simply supported panel at $\Delta T(x)/\Delta T_{cr} = 3$ and $\lambda_l = 1045.6$.

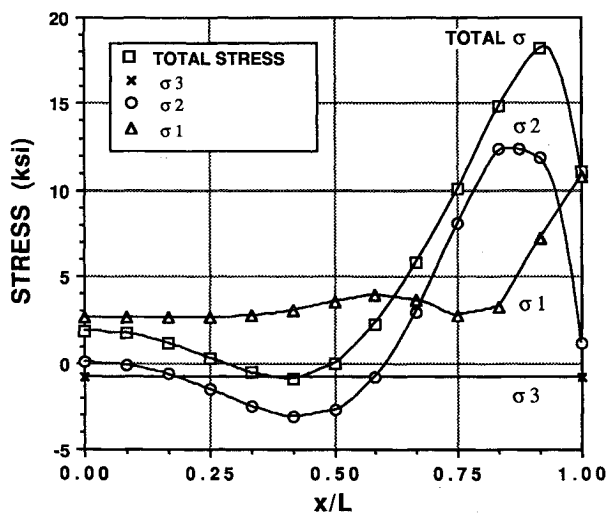

Fig. 10 Stress distributions of a simply supported panel at $\Delta T(x)/\Delta T_{cr} = 3$ and $\lambda_l = 1045.6$.

Static Stability and Flutter Boundaries

Basically, Eq. (6) presents a postbuckling problem with the combined loading of temperature $\Delta T(x)$ and aerodynamic pressure. The static stability boundaries can be found as shown in Fig. 8. Figure 8 is a plot of λ vs $\Delta T(x)/\Delta T_{cr}$, the line CAEG is the boundary which divides the buckled ($\{W\}_s \neq 0$) and the flat ($\{W\}_s = 0$) panel regions. In the region above CAEG, Eq. (6) gives a converged trivial solution $\{W\}_s = 0$ and the panel is flat. The region below the curve CAB, Eq. (6) gives a converged nontrivial solution ($\{W\}_s \neq 0$) and the panel is buckled. Within the area of BAEF bifurcation occurs, Eq. (6) fails to have a converged real solution ($\{W\}_s$ undetermined). In the region of EFG, Eq. (6) gives a converged solution, again the panel is in a buckled equilibrium position ($\{W\}_s \neq 0$). With the examination of the dynamic equation, Eq. (7), it is found that the region below the curve DAB there is no flutter motion (large-amplitude limit-cycle oscillations). The panel remains in the equilibrium position with small-amplitude vibrations. The region above the curve DAEG, Eq. (7) has a converged limit-cycle solution, the panel oscillates from a flat static equilibrium position ($\{W\}_s = 0$), and harmonic motion is obtained. In the region of EFG, Eq. (7) is solved based on a buckled panel, a periodic nonharmonic motion is expected. In the area of bifurcation BAEF, Eq. (7) loses the static solution ($\{W\}_s$ undetermined) and chaotic motion happens.[26] The importance of Eq. (6) is that it not only deals with static solutions, but also determines the nature of dynamic solutions due to the coupling of Eqs. (6) and (7). The chaotic boundaries of a panel could be traced out by applying Eq. (6) with increments of temperature and dynamic pressure. Those boundaries compared well to other analytical solutions.[18,26] In Fig. 8, DA is a critical flutter boundary obtained from Eq. (12) or corresponding to $c = 0$ in Eq. (15). With the increase of dynamic deflection c/h, parallel-like curves could be drawn in the limit-cycle region of DAG. The values at the low ends of those curves bound chaotic motion. In the statically buckled area FEG, a nonharmonic periodic motion should be expected. This is physically due to the nontrivial $\{W_s\}$ and mathematically leads to a quadratic nonlinear term in Eq. (7). The LUM/NTF solution procedure also approximates this quadratic term to a simple harmonic term, thus this approach still gives a harmonic approximation. More accurate methods (time integration,[10] harmonic increments[27]) are needed to analyze the nonharmonic motion but should pay the price of computation time. It is found that at moderately large λ and $\Delta T(x)/\Delta T_{cr}$, some dynamic instability could be reached. At that time Eq. (7) cannot give a converged solution in the iterations. This phenomenon was also observed in the time-integration solution.[10,26]

Dynamic Pressure-Fatigue Life (λ-H) Curve

In the fatigue life analyses, the material ultimate tensile stress is chosen to be 40 ksi. The deflections and total stress distributions for $\Delta T(x)/\Delta T_{cr} = 3$ and $\lambda_l = 1045.59$ are plotted in Figs. 9 and 10, it can be seen that the nonlinear stretching stress plays a significant role. Some of the stresses, frequencies, dynamic pressures, and panel life are listed in Table 1 for reference. The λ-H curves are plotted in Figs. 11 and 12 with different scales. It can be seen that when λ is less than 1350 for $\Delta T(x)/\Delta T_{cr} = 0$, the panel has "infinite" hours of

Table 1 Stresses, frequency f and panel life at various λ_l and $\Delta T/\Delta T_{cr} = 3$ of a simply supported panel

λ_l	c/h	σ_1, ksi	σ_2, ksi	σ_3, ksi	f, Hz	log N	H, h
1086.70	1.62	7.4705	12.2632	−0.8021	274.59	15.4	2.54×10^9
1175.61	1.66	8.0284	13.1795	−0.8021	288.38	10.5	3.05×10^4
1274.53	1.70	8.6341	14.1862	−0.8021	303.29	8.7	459.02
1484.42	1.80	9.8768	16.2787	−0.8021	333.60	6.8	5.25
1694.68	1.90	11.0726	18.3181	−0.8021	362.34	5.6	0.305
1784.21	1.94	11.5736	19.1705	−0.8021	374.15	5.2	0.118

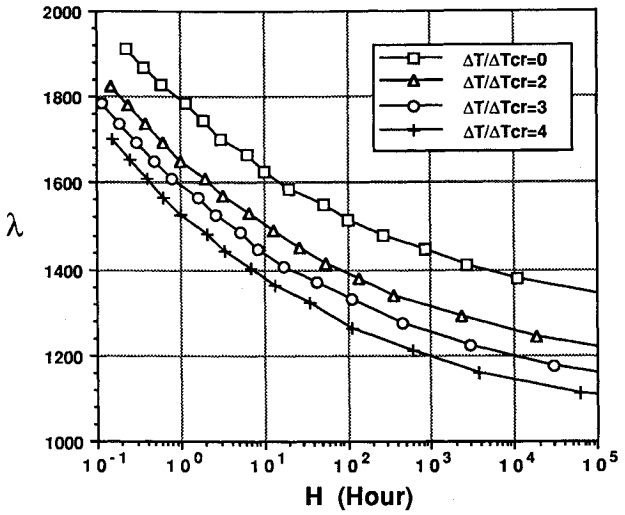

Fig. 11 Limit-cycle dynamic pressure vs fatigue life for a simply supported panel at various $\Delta T(x)/\Delta T_{cr}$ (σ_t = 40 ksi).

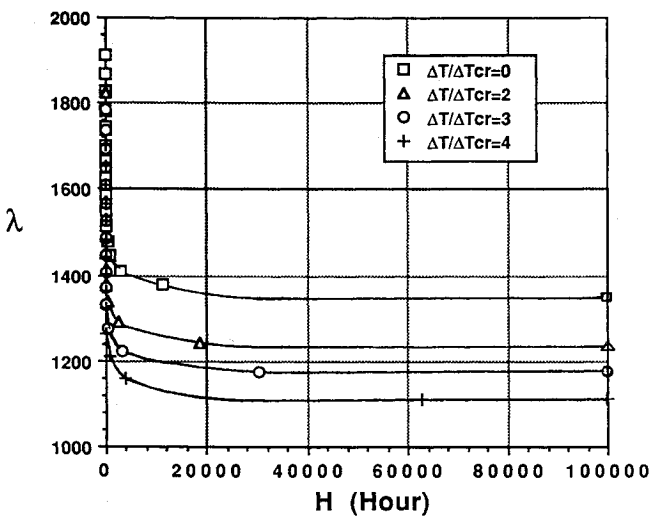

Fig. 12 Limit-cycle dynamic pressure vs fatigue life for a simply supported panel at various $\Delta T(x)/\Delta T_{cr}$ (σ_t = 40 ksi).

life time. This dynamic pressure is called the endurance dynamic pressure λ_e. For the case of $\Delta T(x)/\Delta T_{cr} = 2$, $\lambda_e \cong 1240$; $\Delta T(x)/\Delta T_{cr} = 3$, $\lambda_e \cong 1170$, and $\Delta T(x)/\Delta T_{cr} = 4$, $\lambda_e \cong 1100$. The endurance aerodynamic pressure is useful information for designs of panels. Recall the critical dynamic pressure $\lambda_{cr} = 129$ at $\Delta T(x)/\Delta T_{cr} = 3$ and $\lambda_{cr} = 191$ at $\Delta T(x)/\Delta T_{cr} = 2$, those indicate that the design based on the linear theory is conservative, and the nonlinear panel flutter and fatigue analyses can increase the designing pressure. In addition, the λ-H curves can be used with the well-known Miner's linear cumulative damage theory in estimating panel fatigue life. That is, the percentage of damage D due to dynamic pressures λ_i with h_i hours is accumulated as

$$D = \sum_i \frac{h_i}{H(\lambda_i)}$$

Another interesting result, λ_f can be seen from Fig. 11, i.e., when the dynamic pressure reaches a certain level (e.g., $\Delta T/\Delta T_{cr} = 3$ and $\lambda_f \cong 1800$), the panel would fail immediately, although at that time the total stress is much less than the ultimate strength of 40 ksi (see Table 1).

Conclusions and Remarks

The present finite element formulation and solution procedure is consistent, accurate, and efficient for analyzing nonlinear panel flutter with temperature effects. This procedure could be a useful tool in flutter analysis and design of complex panels.

The two-step decomposition solution procedure is based on a mathematical approach. In the first step, the solution of the equilibrium position gives clear boundaries to determine dynamic characteristics of the panel. The LUM/NTF approximation gives accurate results for the harmonic limit-cycle motion. For a nonharmonic periodic motion, however, this approach will give an equivalent harmonic motion. This is due to the limitation of the frequency domain harmonic assumption.

The λ-H curve is necessary in panel fatigue analysis, since the stresses, frequency, aerodynamic pressure, and temperature are uniquely related in the limit-cycle motions of the panel. The result from fatigue life analysis gives λ_e, which is much larger than critical pressure λ_c. It is concluded that the panel is overdesigned based on linear flutter theory.

Acknowledgment

This work was supported by NASA Langley Research Center under Master Contract Agreement NAS1-18584, Task 38, entitled "Thermal Effects on Nonlinear Panel Flutter."

References

[1]Xue, D. Y., Mei, C., and Shore, C. P., "Finite Element Two-Dimensional Panel Flutter at High Supersonic Speeds and Elevated Temperature," *Proceedings of 31st Structures, Structural Dynamics and Materials Conference*, Long Beach, CA, April 1990, pp. 1464–1475.

[2]Fung, Y. C., "The Flutter of a Buckled Plate in a Supersonic Flow," Guggenheim Aeronautical Lab., California Inst. of Technology, Air Force Office of Scientific Research TN 55-273, Pasadena, CA, 1955.

[3]Shideler, J. L., Dixon, S. C., and Shore, C. P., "Flutter at Mach 3 Thermally Stressed Panels and Comparison with Theory for Panels with Edge Rotational Restraint," NASA Langley Research Center, TN D-3498, Hampton, VA, Aug. 1966.

[4]Dowell, E. H., "Panel Flutter: A Review of the Aeroelastic Stability of Plates and Shells," *AIAA Journal*, Vol. 8, March 1970, pp. 385–399.

[5]Reed, W. H., Hanson, P. W., and Alford, W. J., "Assessment of Flutter Model Testing Relating to The National Aero-Space Place," NASA Langley Research Center, NASP CR-1002, Hampton, VA, July 1987.

[6]Eastep, F. E., and McIntosh, S. C., "Analysis of Nonlinear Panel Flutter and Response Under Random Excitation or Nonlinear Aerodynamic Loading," *AIAA Journal*, Vol. 9, March 1971, pp. 411–418.

[7]Eslami, H., "Nonlinear Flutter and Forced Oscillations of Rectangular Symmetric Cross-Ply and Orthotropic Panels Using Harmonic Balance and Perturbation Method," Ph.D. Dissertation, Old Dominion Univ., Norfolk, VA, 1987.

[8]Morino, L., "A Perturbation Method for Treating Nonlinear Panel Flutter Problems," *AIAA Journal*, Vol. 7, March 1969, pp. 405–410.

[9]Kuo, C. C., Morino, L., and Dugundji, J., "Perturbation and Harmonic Balance Methods for Nonlinear Panel Flutter," *AIAA Journal*, Vol. 10, Nov. 1972, pp. 1479–1484.

[10]Dowell, E. H., "Nonlinear Oscillations of a Fluttering Plate," *AIAA Journal*, Vol. 4, July 1966, pp. 1267–1275.

[11]Ventres, C. S., and Dowell, E. H., "Comparison of Theory and Experiment for Nonlinear Flutter of Loaded Plates," *AIAA Journal*, Vol. 8, Nov. 1970, pp. 2022–2030.

[12]Mei, C., and Rogers, J. L., Jr., "Application of NASTRAN to Large Deflection Supersonic Flutter of Panels," NASA TM X-3428, Oct. 1976, pp. 67–97.

[13]Mei, C., "A Finite Element Approach for Nonlinear Panel Flutter," *AIAA Journal*, Vol. 15, Aug. 1977, pp. 1107–1110.

[14]Rao, K. S., and Rao, G. V., "Large Amplitude Supersonic Flutter of Panels with Ends Elastically Restrained Against Rotation," *Computers and Structures*, Vol. 11, March 1980, pp. 197–201.

[15]Han, A. D., and Yang, T. Y., "Nonlinear Panel Flutter Using High-Order Triangular Finite Elements," *AIAA Journal*, Vol. 21, Oct. 1983, pp. 1453–1461.

[16]Sarama, B. S., and Varadan, T. K., "Non-Linear Panel Flutter by Finite Element Method," *AIAA Journal*, Vol. 26, May 1988, pp. 566–574.

[17]Gray, C. E., Jr., Mei, C., and Shore, C. P., "A Finite Element Method for Large-Amplitude Two-Dimensional Panel Flutter at Hypersonic Speeds," *AIAA Journal*, Vol. 29, Feb. 1991, pp. 290–298.

[18]Houbolt, J. C., "A Study of Several Aerothermoelastic Problems of Aircraft Structure in High-Speed Flight," Ph.D. Dissertation, Swiss Federal Inst. of Technology, Zurich, Switzerland, 1958.

[19]Yang, T. Y., and Han, A. D., "Flutter of Thermally Buckled Finite Element Panels," *AIAA Journal*, Vol. 14, July 1976, pp. 975–977.

[20]Schaeffer, H. G., and Heard, W. L., Jr., "Flutter of a Flat Plate Exposed to a Nonlinear Temperature Distribution," *AIAA Journal*, Vol. 3, Oct. 1965, pp. 1918–1923.

[21]Qin, J., Gray, C. E., Jr., and Mei, C., "A Vector Unsymmetric Eigenequation Solver for Nonlinear Flutter Analysis on High-Performance Computers," *Proceedings of 32nd Structures, Structural Dynamics and Materials Conference*, Baltimore, MD, April 1991, pp. 1971–1980; see also *Journal of Aircraft* (to be published).

[22]Heywood, R. B., "Designing Against Fatigue," Chapman and Hall, London, 1962.

[23]Ashley, H., and Zartarian, G., "Piston Theory—A New Aerodynamic Tool for the Aeroelastician," *Journal of Aeronautical Sciences*, Vol. 23, No. 12, Hampton, VA, 1956, pp. 1109–1118.

[24]Kordes, E. E., Tuovila, W. J., and Guy, L. D., "Flutter Research on Skin Panels," NASA Langley Research Center, TN D-451, Sept. 1960.

[25]Rudder, F. F., Jr., and Plumblee, H. E., Jr., "Sonic Fatigue Design Guide for Military Aircraft," Air Force Flight Dynamics Lab. TR-74-112, Wright-Patterson AFB, OH, May 1975.

[26]Dowell, E. H., "Flutter of a Buckled Plate as an Example of Chaotic Motion of a Deterministic Autonomous System," *Journal of Sound and Vibration*, Vol. 85, No. 3, 1985, pp. 333–344.

[27]Lau, S. L., Cheung, Y. K., and Wu, S. Y., "Nonlinear Vibration of Thin Elastic Plates," American Society of Mechanical Engineers, *Journal of Applied Mechanics*, Vol. 51, 1984, pp. 837–851.